Chapter

Structure and Properties of Alkaline Cement and Concrete and Choice of Factors That Affect Service Life

Oles Lastivka

Abstract

The chapter covers the results of influence of changes in proportions between Portland cement and slag content, along with different quantities of alkali components in the cement systems on their heat of hydration and the effect of this during their hardening on character of internal stresses development and crack opening in concrete. The correlation between heat of hydration of the cements during hardening, strength of the concrete and stress development, and the dependence of this relationship on technical and technological factors were received. A new structure-based model for the durability (cracking) assessment of the alkaline cement concrete with heat of hydration and deformation properties during hardening as the input was received.

Keywords: alkaline cement, granulated blast-furnace slag, sodium carbonate, sodium metasilicate pentahydrate, concrete, chemical shrinkage, internal stress, modeling deformation

1. Introduction

One of the key objectives of contemporary material science and engineering is to develop new types of effective cement and concrete, which ensure a synthesis of long-lasting artificial conglomerates with high physical, mechanical characteristics and performance. It is well known that concrete is a proven and reliable building material, which is used all over the world in many types of buildings. Special concretes are used for constructing contemporary high-rise buildings and their structural elements, which are expected to have high performance in the service environment, particularly in urban conditions. However, rather high cement contents (400–500 kg/m^3) and low water-cement ratios in such concretes can result in crack formations due to thermal stresses and shrinkage deformations, thereby lowering the durability of these structures.

It is known that thermal stresses in concrete depend on the exothermic nature of cement hydration and temperature gradient between the core and surface of structural elements [1]. The temperature gradients result in deformations, which, due to space limitations, can lead to compressive stresses in one part of the structure and

stretching in another part. If these stresses exceed the limit of stretching strength, then cracks will appear and expand over the structure's surface. The possibility of forecasting and controlling heat evolution in concrete during hardening allows avoiding the formation of temperature cracks [2]. This explains the necessity of an enhanced study of the concrete's hardening processes at the early stages, depending on a set of recipe and technological factors.

One of the methods of avoiding the thermal crack formation in concrete structures is the use of cements with active mineral additives, such as fly ash and silica fume. These materials result in an increase in strength due to pozzolanic reaction, reduction in heat evolution during cement hydration and improvement in the concrete durability [3–5]. As before-mentioned, Portland cement remains the main cementitious material in concrete for creating such high-strength concretes, which, however, has certain disadvantages in its production, including high energy consumption and adverse environmental effects. In this respect, the development of technologies and research projects aimed at shortening greenhouse gas emissions and reducing energy consumption becomes essential [6].

From this point of view, alkaline cements developed by the scientific school of Prof. Glukhovsky in Ukraine are one of the most advanced materials. These are represented by five types in accordance with the national standard of Ukraine. The important characteristic of such cements is the possibility of using up to 90% of industrial wastes as the raw material while ensuring not only the strength and durability that are normally obtained with traditional Portland cements but also that is commonly associated with high-strength cements. Such cement systems allow a reduction in energy consumption during cement production, decrease the pollution of the environment and protect natural resources.

The prospects of using alkaline slag cement as one of the types of alkali cement in concretes have been confirmed by more than 50 years of research experience in this area [7–9]. Its use has been found to produce concretes with low heat evolution, high early strength, better dimensional stability and long-term durability. However, the alkaline slag Portland cement has not been widely investigated as part of the system of cements described earlier.

In order to ensure the long-term durability of concretes based on alkali slag cement, an investigation was carried in which the development of its early structure formation was studied in terms of heat of hydration, deformation and crack formation. The mix compositions were decided based on information available in the existing literature on its technical and technological properties, with the slag content varying from 50 to 100% of the total binder content and a variable content of alkali component in the cement.

2. Materials and methods

2.1 Mix compositions

Table 1 reports the composition of cement mixes investigated in this chapter. The alkaline slag Portland cement (ASPC) used in this research was manufactured with the ground granulated blast-furnace slag (GGBS) content varying from 50 to 88% and the remainder consisting of Portland cement (CEM I). Another set of experiments was carried out with ground Portland cement clinker used to replace CEM I at a GGBS content of 50%. A third set of mixes was termed alkaline slag cement (ASC), which consisted of 100% GGBS content and alkaline activator materials (see the section on materials for details of the alkaline materials used), in accordance with reference [10]. CEM II/A-S 42.5 (PC) was used as a control

Reference*	Composition of cement, %			Chemicals % by weight of cement**			W/C
	GGBS	CEM I	Portland cement clinker	Na_2SiO_3 **$5H_2O$	Na_2CO_3	LST	
SPSi3C0	50	50	—	3	—	0.8	0.5
SPSi0C2.5	50	50	—	—	2.5		
SCSi3C0	50	—	50	3	—		
SCSi0C2.5	50	—	50	—	2.5		
SPSi3.5C0	69	31	—	3.5	—		
SPSi0C3	69	31	—	—	3		
SPSi0C4	88	12	—	—	4		
SSi7C0	100	—	—	7	—		
SSi0C5.5	100	—	—	—	5.5		
SSi2C5	100	—	—	2	5		
PC	CEM II/A-S 42.5						

**References for cementitious materials are based on the following notations: first the cementing materials, then the silicate content, followed by the carbonate content. PC stands for the CEM II/A-S control.*
***The content of chemicals taken over 100% of the composition of cement.*

Table 1
Experimental variables and mix compositions.

composition. For all 11 mixes, the water-to-cement ratio was 0.5 and the sand-to-cement ratio was 3.

Details of the full set compositions of concrete mixes investigated are given in **Table 2**. The nine compositions of concrete mixes were as follows: cement – 400 kg/m^3, sand – 680 kg/m^3, aggregate fraction 5 to 10 mm – 360 kg/m^3 and fraction 10 to 20 mm – 790 kg/m^3. Changing composition of cement in concrete mixes was an experimental variable factor.

2.2 Materials

In both ASPC and ASC, granulated blast-furnace slag was used (basicity module Mb = 1.1, 95% of glass phase). CEM I and Portland cement clinker were used as the

Reference	Composition of cement, %		Chemicals % by weight of cement			Cement kg/m^3	Aggregate fraction, kg/m^3		Sand, kg/m^3
	GGBS	CEM I	Na_2SiO_3*$5H_2O$	Na_2CO_3	LST		5–10 mm	10–20 mm	
SPSi3C0	50	50	3	—	0.8	400	360	790	680
SPSi0C2.5	50	50	—	2.5					
SPSi3.5C0	69	31	3.5	—					
SPSi0C3	69	31	—	3					
SPSi0C4	88	12	—	4					
SSi7C0	100	—	7	—					
SSi0C5.5	100	—	—	5.5					
SSi2C5	100	—	2	5					
PC	CEM II/A-S 42,5								

Table 2.
Compositions of concrete mixes.

Components	Content of oxides, %									
	SiO_2	Al_2O_3	Fe_2O_3	CaO	MgO	MnO	Na_2O	SO_3	K_2O	TiO_2
GGBS	35.84	11.32	0.39	38.79	8.66	0.50	0.23	1.58	0.60	0.96
Portland cement clinker	22.06	5.49	2.98	64.95	1.83	0.06	0.22	0.6	0.52	0.29
CEM I	21.5	6.9	2.74	63.6	1.7	0.08	0.18	1.7	0.51	0.35
CEM II/A-S	21.7	5.8	3.3	59.0	2.4	0.88	0.45	2.6	0.40	0.2

Table 3.
The chemical composition of cement components.

components of ASPC. The control mix consisted of 100% CEM II/A-S 42.5. The chemical composition of cement components is reported in **Table 3**.

The alkaline components used in ASPCs were sodium carbonate (Na_2CO_3) and sodium metasilicate pentahydrate (Na_2SiO_3*$5H_2O$). The ASPC was produced as an "all in one" product (dry mix of all components), along with sodium lignosulfonate (LST) admixture to ensure setting time and strength. To assist inter-grinding of slag and clinker, etylhidrosyloksan polymer was used, which prevented absorption of moisture by cement and maintained the properties of cement.

The grinding of ASC was done to obtain a fineness characterized by a specific surface area of 470 m^2/kg. For Portland cement clinker, the fineness, characterized by the specific surface of 430 m^2/kg, was ensured with the use of the grinder and the air-jet sieve shown in **Figure 1**.

3. Test methods

3.1 X-ray diffraction (XRD) analysis

Paste specimens weighing about 5 g were made from 5φ × 5 cm test cylinders, and then, they were wrapped in polythene sheets at 7 and 28 days of curing. The curing temperature was 20 (± 2)°C. After curing, the specimens were put into bottles filled with pure isopropanol in order to stop their hydration. Then, the specimens were filtered from the isopropanol and dried in the desiccators in a vacuum. Part of the dried samples was ground in an agate mortar. Particles passing a 63-μm sieve were used for X-ray diffraction. The X-ray diffraction analysis was

Figure 1.
Laboratory grinder and air-jet sieve for collecting ground PC clinker.

conducted using an X-ray diffractometer (Bruker D2 Phaser Benchtop) with Cu Ka1 radiation and a 2Θ scanning range of 7–60°. The XRD scans were performed at a 0.05° interval per second.

3.2 Calorimetry

The chemical reactions involved in cement hydration are globally exothermal, and the associated heat output can be obtained either numerically or experimentally. Numerical prediction of the heat of hydration of cement requires a knowledge of its chemical composition, which in turn can be used for calculating the percentages of the clinker components C_3S, C_2S, C_4AF and C_3A according to Bogue's formula or similar [11, 12]. The heat generation potential of each of these components has been thoroughly studied in the past, and so currently several well-known models exist [12, 13]. However, for composite cements, numerical predictions of any of these models often fail due to the complex chemical interactions that can occur [14]. Therefore, heat of hydration of alkaline cements is determined using experimental tests based on the isothermal calorimeter method. In this test, an eight-channel isothermal calorimeter TAM Air was used, and tests were carried out at a temperature of 20 (± 2)°C and using pastes made of 0.4 water-cementitious material ratio. The heat of hydration of cement was determined during 7 days of hardening.

3.3 Chemical shrinkage

The method for studying chemical shrinkage of cement pastes is normally done according to ASTM C1608 [15]. It consists of a flask that contains the paste, on top of which a capillary is connected and filled with water (**Figure 2**). The water level is monitored using a webcam connected to a laptop. A few drops of oil with a red colorant are added to the water in the capillary to avoid evaporation of the water. The colored oil drops are also used as tracers in the image analysis of the pictures of the capillary taken with the webcam. The flasks are immersed in a thermostatic water bath and maintained at 20°C. Chemical shrinkage of cement is investigated within 28 days of curing.

3.4 Compressive strength

The test was carried out according to BS EN 196-1:2005. Compressive strength of mortars specimens was determined by three prismatic specimens 40 × 40 mm in

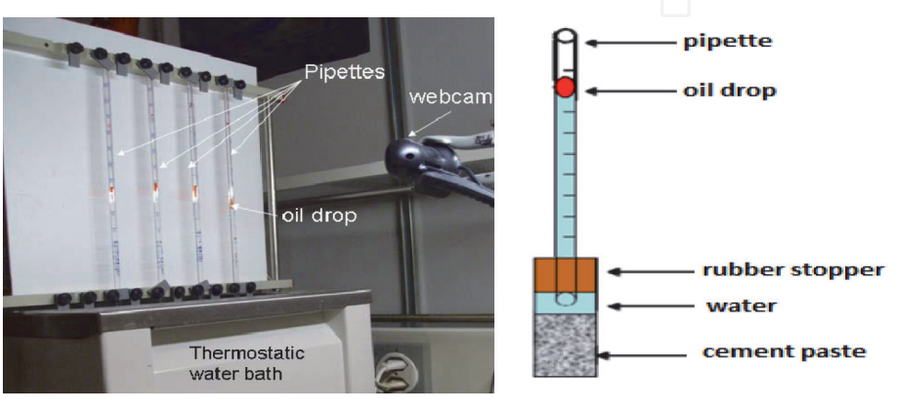

Figure 2.
Setup developed for the measure of chemical shrinkage (left) and the device used to measure the change in volume by means of dilatometry (right).

cross section and 160 mm in length after hardening at temperature 20 (± 2)°C and humidity 95 (± 5)% at the age of 2, 7 and 28 days for each mix. Steam room with temperature and humidity controlled is used for curing the various specimens of mortars. The mortar specimens were cured immediately after casting, demolded the next day and cured at room temperature until compressive strength test. The compressive strength result represents the average of three tests with an error deviation of less than 7%.

The compressive strength of the concrete specimens was determined by crushing three cubes of 100 mm size after hardening at temperature 20 (± 2)°C and humidity 95 (± 5)% at the age of 7, 14 and 28 days for each mix. The test was carried out according to BS EN 12390–3:2009. Constant rate of loading of specimens was within the range 0.4 MPa/s ($N/mm^2 \cdot s$).

3.5 Drying shrinkage

The drying shrinkage tests were carried out following the procedures in ISO 1920-8-2009 [16]. Gauge studs of stainless steel were placed at the end surfaces of the specimens, with each partially embedded the sample for 15 mm and the line joining them coinciding with the main axis of the sample. Shrinkage deformations were evaluated using concrete specimens with size 75 × 75 × 280 mm, which were demolded 24 h after casting and moist cured at temperature 20 (± 2)°C and humidity 95 (± 5)% until the age of 2 days. After the moist curing period, the specimens were stored at a temperature of approximately 20 (± 2)°C and relative humidity of 60 (± 5)% until the completion of the test. The first measurement of drying shrinkage of concrete specimens was done at the age of 48 (± 0.25) h.

3.6 Creep deformation

The creep tests were carried out following the procedures in ISO 1920-9-2009 [17]. Creep deformations were evaluated using concrete specimens of cylinders with size 100 × 100 × 400 mm, which were demolded 24 h after casting, and moist cured at temperature 20 (± 2)°C and humidity 95 (± 5)% until the age of 7 days. After the moist curing period, the specimens were stored at a temperature of approximately 20 (± 2)°C and relative humidity of 60 (± 5)% until the completion of the test. The first measurement of creep deformation of concrete occurred at the age of 14 days.

4. Description of the main results

4.1 Cement characterization

The investigations with the use of CEM I were carried out in order to evaluate the possibility of substituting clinker additive for CEM I in the composition of alkaline cements. The system “slag – CEM I - alkaline component” was considered, which included 50–100% of slag during the type change and the loss of alkaline component and CEM I (**Table 4**). It has been demonstrated that the substitution of Portland cement clinker for CEM I in the composition of alkali cement does not deteriorate the key properties of the binders. Depending on the slag and CEM I contents when using sodium carbonate within the limits of 2.5–5%, the cement is characterized by the beginning of setting at ≥55 minutes, and the strength of 9.2–19.7 MPa after 2 days and 40–46 MPa after 28 days. When using the sodium metasilicate, the beginning of setting is extended, and the cement strength is

Reference*	Composition of cement, %						Initial setting time, min	Strength, MPa, at different ages in days		
	GGBS	CEM I	Portland cement clinker	$Na_2SiO_3*5H_2O$	Na_2CO_3	LST		2	7	28
SPSi3C0	50	50	—	3	—	0.8	60	19.7	35.7	45.8
SPSi0C2.5	50	50	—	—	2.5		55	18.2	33.2	44.5
SCSi3C0	50	—	50	3	—		65	20.1	34.9	46.1
SCSi0C2.5	50	—	50	—	2.5		55	18.0	33.8	43.2
SPSi3.5C0	69	31	—	3.5	—		70	15.4	33.0	45.3
SPSi0C3	69	31	—	—	3		60	14.1	32.5	42.4
SPSi0C4	88	12	—	—	4		65	12.5	29.4	41.8
SSi7C0	100	—	—	7	—		60	11.8	31.6	43.7
SSi0C5.5	100	—	—	—	5.5		60	9.2	28.1	39.8
SSi2C5	100	—	—	2	5		65	11.5	32.9	43.9
PC	CEM II/A-S 42.5						115	19.4	34.2	43.1

**References for cementitious materials are based on the following notations: first the cementing materials, then the silicate content, followed by the carbonate content. PC stands for the CEM II/A-S control.*

Table 4.
Setting time and strength of alkaline cement and CEM II/A-S.

increased at an early age within the whole range of the slag component content. At the same time, the use of the combination of sodium metasilicate pentahydrate with sodium carbonate ash as alkali components allows to extend the beginning of setting and to increase the cement strength.

It is possible to assert that with the increase of the slag component content, the alkaline cement strength decreases at the early hardening stages as compared with the PC. However, after 7 days of hardening, the strength indices are raised to the level of PC.

So, the compositions of alkaline cement with the range of slag content (50–100%) and CEM I (12–50%) are obtained, which comply with the requirements [10] in accordance with the investigated properties and are related to class 42.5 cements.

4.2 Heat of hydration for cement

The thermodynamic calculations [18] show that the basicity of hydration products and the hydration heat depend on the output Portland cement phases. The decrease of the number of Ca^{2+} ions and the ratios of CaO/SiO_2 and CaO/Al_2O_3 in the calcium silicate and aluminate groups reduce the importance of hydration heat effects. These thermodynamic provisions are confirmed by the experimental investigations of alkaline cements (**Figures 3** and **4**). For example, the high basicity of PC facilitates the formation of $Ca(OH)_2$, ettringite and highly basic calcium silicate hydrates at the initial hardening stages (**Figure 3**). Their formation is accompanied by significant heat effects - the value of hydration heat reaches 400 J/g (**Figure 4**). At the same time, the lowering of the dispersed phase basicity in alkaline cements at the expense of CaO facilitates the increase of forming the low basic silicate hydrates in the composition of hydration products. The heat of their formation is lower as

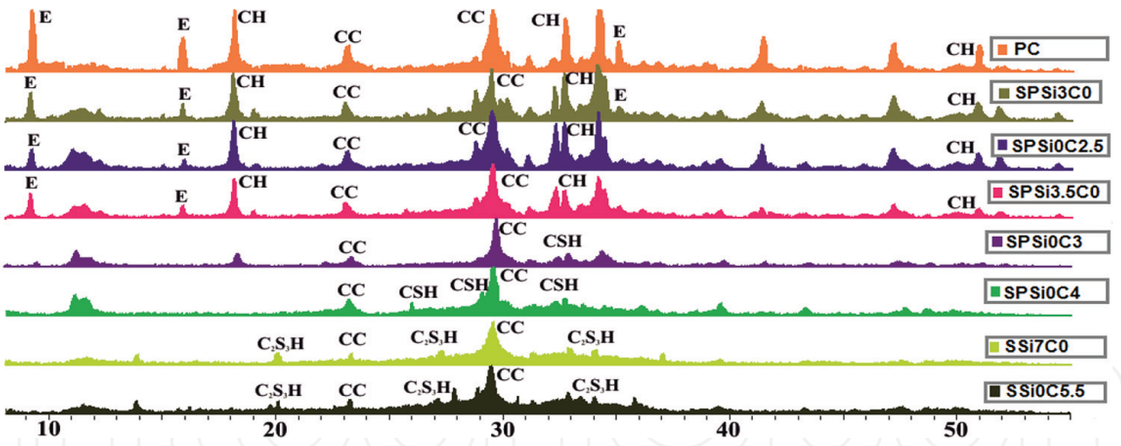

Figure 3.
XRD patterns of alkaline cement and CEM II/A-S after 7-day hydration. ***Notations:*** *PC-CEM II/A-S control, S—Slag, P—Portland cement, Si—Silicate, C—Carbonate.*

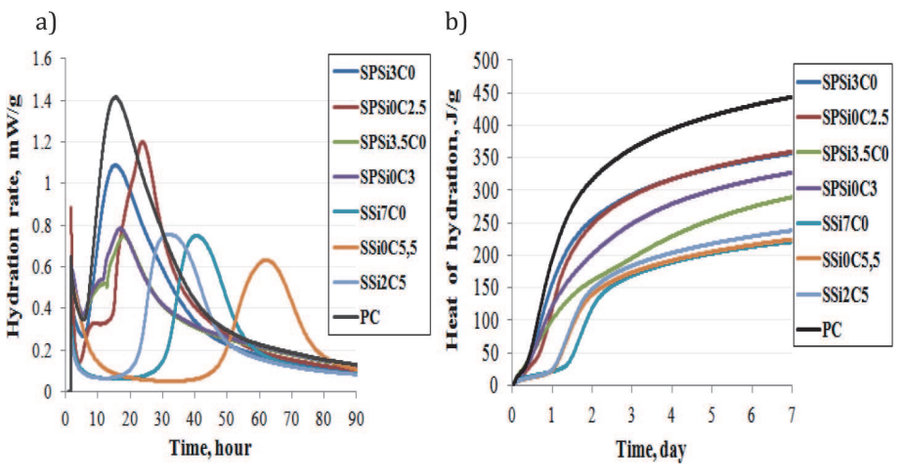

Figure 4.
Influence of alkaline cement and CEM II/A-S on the hydration rate (a) and released heat of hydration (b).

compared with the heat of highly basic silicate hydrates, which makes up 200–350 J/g. In this respect, the hydration heat of alkaline cements is lower as compared with the hydration heat of PC.

The intensity and completeness of heat of hydration during hydration of binders reduce progressively with the decrease of CaO content at the expense of Portland cement (**Figure 4**). The value of the first exo-effect varies from 1.4 mW/g for PC to 0.6 mW/g for ASC. The duration of induction period increases from 10 h for PC to 60 h for ASC.

The substitution of sodium carbonate with sodium metasilicate and the mixture of soda with sodium metasilicate was investigated in order to evaluate the impact of alkaline component nature on the value of specific heat of hydration. It has been demonstrated that alkaline cement (sodium carbonate in the amount of 5.5% has been added to its composition) is characterized with the lowest specific heat of hydration indices. The specific heat of hydration is 210 J/g after 7 days, while for another two compositions, the specific heat of hydrations is 230–240 J/g.

The continuous cooling transformation investigations conducted helped specify that irrespective of slag content, nature and quantity of alkaline component, the alkaline cement is characterized with low specific heat of hydration indices, while high strength indices are achieved both at the early hardening stages and in the standard age of 28 days.

4.3 Chemical shrinkage of cement pastes

The volumetric changes in the cement stone gel, which depend on the system mineralogical composition, cement grinding fineness, conditions and time of hardening, are the key reasons for chemical shrinkage of the binding systems. The shrinkage value at the micro-level depends, first of all, on the ratio of crystalline and gel phases in hydration products of the binders on the density of these compounds. The results of chemical shrinkage are represented in **Figure 5**.

It is shown that the chemical shrinkage of the PC pastes is higher as compared with the alkaline cements. For example, PC composition pastes are characterized by shrinkage within the limits of 0.82 mL/g after 28 days of hardening. When using the alkaline cement SSi0C5.5 composition, the shrinkage deformations decrease down to 0.41 mL/g. The deformations decrease with the increase of slag content and the relevant increase of alkaline composition in the cement. For example, the shrinkage deformations are equal to 0.65 mL/g in the system, with 50% slag and 2.5% sodium carbonate content. The shrinkage deformations decrease down to 0.40–0.43 mL/g with the increase of slag content up to 88–100% and the relevant increase of alkaline component in the cement. At the same time, the substitution of sodium carbonate with sodium metasilicate in the cement composition reduces shrinkage deformations of the binders down to 0.38 mL/g.

Therefore, the use of alkaline cement systems facilitates the decrease of chemical shrinkage indices by 15–65% as compared with the PC-based system.

4.4 Concrete strength

The heavy concrete composition (see Section 2), which includes the binder in an amount of 400 kg/m^3, was used to determine the effect of cement composition on the compressive strength of concrete.

The investigation results (**Table 5**) show that with the increase of slag content in the cement, and the concrete strength is reduced by 5–15% in the early stage. However, after 14 days of hardening, the concrete strength, based on alkaline cement within the whole range of the slag component content (50–100%), reaches or becomes equal to the strength of concrete with PC. After 28 days of hardening the concrete strength, based on alkaline cement, equals 48.8–51.4 MPa.

It is worth noting that in accordance with the results obtained, it is possible to identify decreasing early strength of concretes and reduction of specific heat of hydration indices with the increase of slag component in cement composition. Therefore, the increase of slag component is accompanied by improvement of one

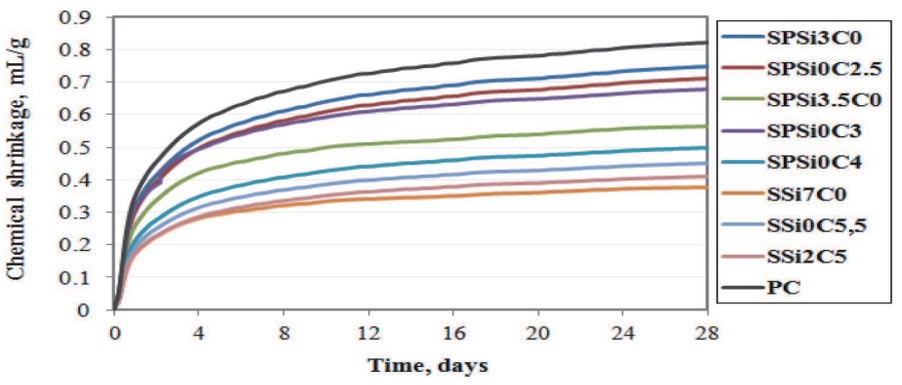

Figure 5.
Chemical shrinkage of alkaline cement and CEM II/A-S.

Reference	Composition of cement, %					W/C	Concrete strength, MPa, at different ages in days		
	GGBS	CEM	Na_2SiO_3*$5H_2O$	Na_2CO_3	LST		7	14	28
SPSi3C0	50	50	3	—	0.8	0.41	35.1	41.4	51.4
SPSi0C2.5	50	50	—	2.5		0.41	36.5	41.5	48.2
SPSi3.5C0	69	31	3.5	—		0.41	34.7	42.3	49.5
SPSi0C3	69	31	—	3		0.41	33.6	40.9	48.4
SPSi0C4	88	12	—	4		0.40	31.7	41.3	49.8
SSi7C0	100	—	7	—		0.40	30.7	39.4	47.7
SSi0C5.5	100	—	—	5.5		0.41	28.9	38.8	45.1
SSi2C5	100	—	2	5		0.40	31.2	40.2	48.8
PC	CEM II/A-S 42.5					0.43	34.6	41.1	47.6

Table 5.
Concrete strength.

index (reduction of specific heat of hydration) and deterioration of the other (decrease of the early strength). That is why it is necessary to search the optimal cement type for concrete in structures, by considering the quantitative changes in combination of properties. This can be done by considering an index—Coefficient of constructive heat (Cch) [19]:

$$Cch = R_{7(28)}/Q_7, \tag{1}$$

where $R_{7(28)}$—compressive strength at 7 and 28 days; Q_7—heat of hydration at 7 days.

Actually, the Cch attests the efficiency of using the binder: The more the strength and the less the heat of hydration, the more are the Cch values and the more the effectiveness of cement use in concrete.

The Cch comparison for the concretes based on alkaline cements after 28 days of hardening (**Figure 6**) testifies to the effectiveness of slag content in the cement within the range of 50–100%, with which the factor gets the values within the range of 1.4–1.8, while for the PC the factor is 1.2.

4.5 Modeling of internal stress in concrete

The thermal stress condition of the concrete was investigated by means of forecasting method using ELCUT software solution [20]. A cast *in situ* wall 3 m wide, 50 m long and 7 m high, concreted at an ambient temperature of 20°C, was used as a block sample for the simulation. The thermal and physical indices of concrete (heat capacity, heat conductivity, heat transfer factor) are accepted in accordance with references and regulatory data [21]. The following tolerances are approved for minimizing the crack formation: The allowable temperature difference between the structure's core and side surface (horizontal gradient) is 18°C; the one between the structure's core and upper/lower surfaces (vertical gradients) is 16°C.

The following relationship was used for modeling the heat evolution of concrete:

$$Q(t) = Q * \left(1 - e^{-kQ} * e^{-nQ}\right. . \tag{2}$$

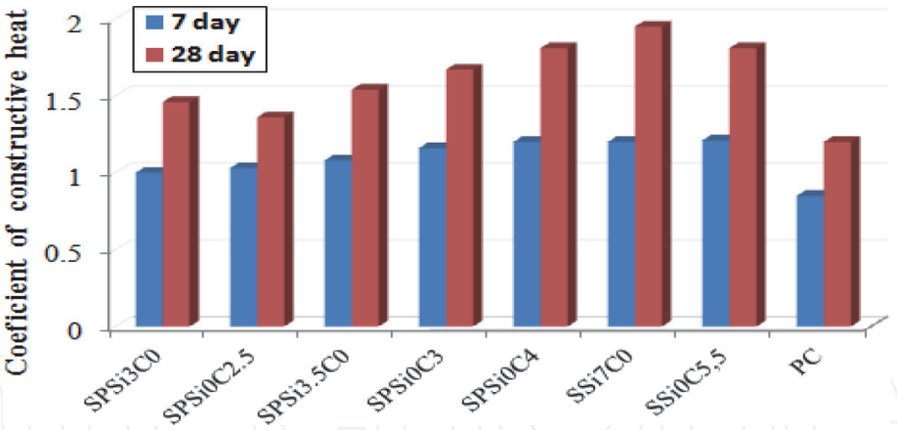

Figure 6.
Dependence Cch from cement composition.

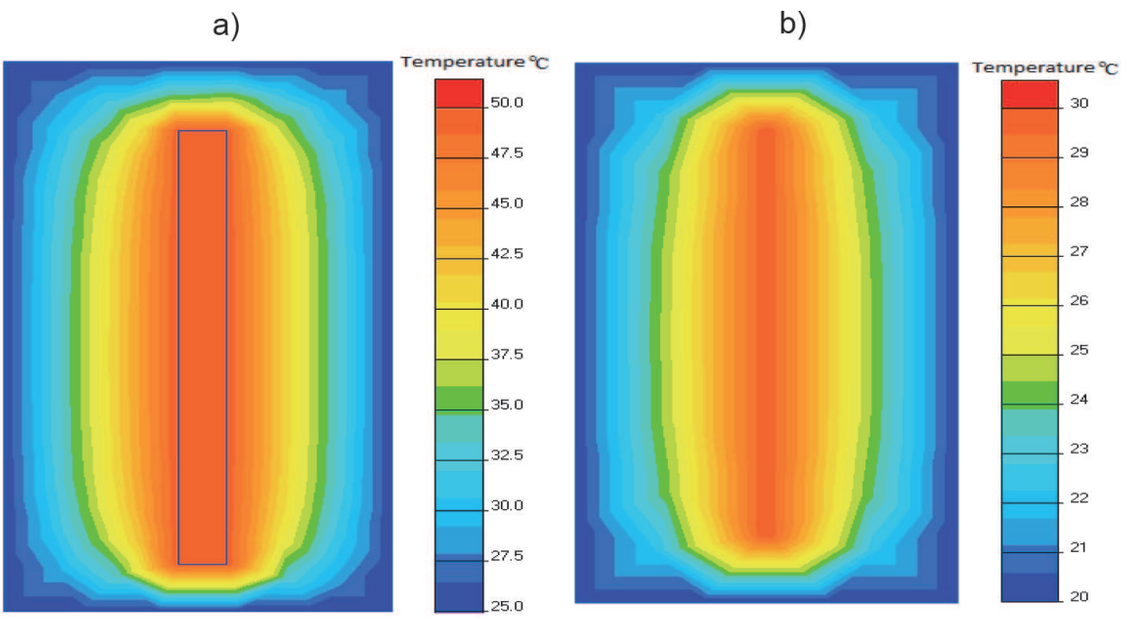

Figure 7.
Temperature distribution of modeled concrete block based on PC (a) and SSi7Co (b).

where Q—integral heat evolution of concrete (kJ/m^3); τ—time (h); k_Q i n_Q—dimensionless coefficients determined method Monte Carlo. Eq. (2) was used for modeling of temperature and the resulting stresses in the concrete block.

PC and SSi7C0 compositions (**Table 4**) of the concrete are selected for simulating temperature distributions along the wall. The simulation results are shown in **Figures 7** and **8**.

The results show that when using PC, the concrete with the maximum heat evolution, the maximum structure's core temperature is 50°C. At the same time, the core temperature of the structure from SSi7C0 composition of the concrete is 30°C. The temperature gradient between the core and vertical surface varies from 25°C for the concretes with maximum heat evolution to 10°C for the concrete with minimum heat evolution (SSi7C0 composition).

The stress envelopes, which occur under the relevant temperatures, were built on the basis of the calculated temperature fields. The following concrete characteristics were taken into account for building the envelopes: Young's modulus E = 30 GPa; Poisson's ratio = 0.3; shear modulus G = 12 GPa.

In accordance with the stress envelopes (**Figure 8**), the maximum stretching stresses occur at the upper and side block planes; at the same time, the block center

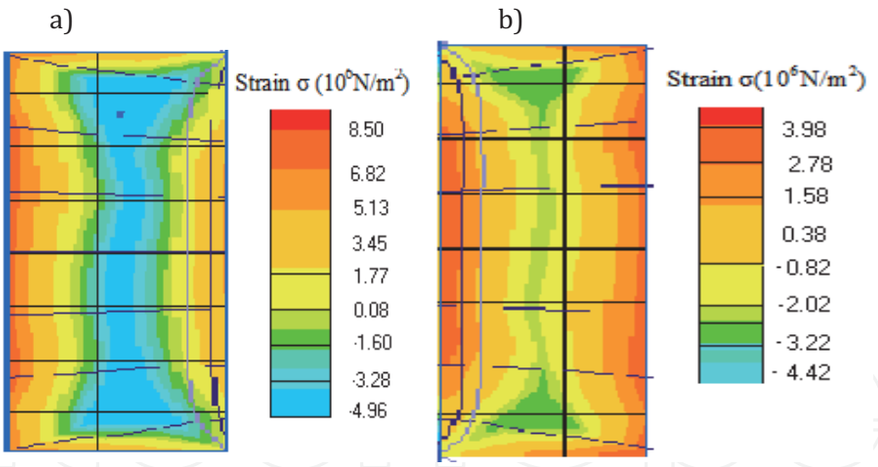

Figure 8.
Internal stresses of modeled concrete blocks based on cement PC (a) and SSi7Co (b).

is compressed. The concrete (SSi7C0 composition) with the minimum heat evolution allows to reduce twice both stretching and compressing stresses in the concrete block as compared with the similar stresses for concrete with the maximum heat evolution (PC composition). Therefore, the maximum stretching stresses are approximately 4 MPa for SSi7C0 composition of the concrete; at the same time, they are equal to 8.5 MPa for PC composition of the concrete.

4.6 Drying shrinkage of the concrete

The drying shrinkage deformation is the most widespread type of shrinkage, which occurs in the material that is already hardened, and which can cause cracking in concrete, for example, along the prestressed reinforcement, or in the products with a large open surface, and relevantly can deteriorate the quality of structures and their durability. The shrinkage appearance is stipulated, first of all, by water removal from the cement gel, which is not bound by molecular forces with a hard phase [22]. The investigation results of drying shrinkage, as well as mass losses of concrete samples, are shown on the basis of investigated cements in order to determine the concrete deformation condition (**Figure 9**).

It has been identified that the concrete samples, based on the PC and alkaline cements, are characterized by almost the same indices of shrinkage deformation and mass loss after 28 days of hardening. For example, when using SPSi3C0 composition of the concrete, the shrinkage makes up 0.064 mm/m after 28 days of hardening. The shrinkage deformations increase up to 0.072 mm/m with the increase of slag content up to 69% in the cement. However, the shrinkage decreases down to 0.061 mm/m when using the cement with maximum slag content. As a comparison, the shrinkage deformations of concrete, based on the PC, make up 0.065 mm/m.

4.7 Creep deformation of the concrete

The creep mechanism of concrete is rather difficult. It is not fully known until now. The most probable creep mechanism can be explained by water removal from C-S-H gel and cracking due to application of loads. Because the cement component of concrete makes a significant impact on the creep, the impact of the composition of alkaline cement on the formation of concrete creep deformation is specified. The results are shown in **Figure 10**.

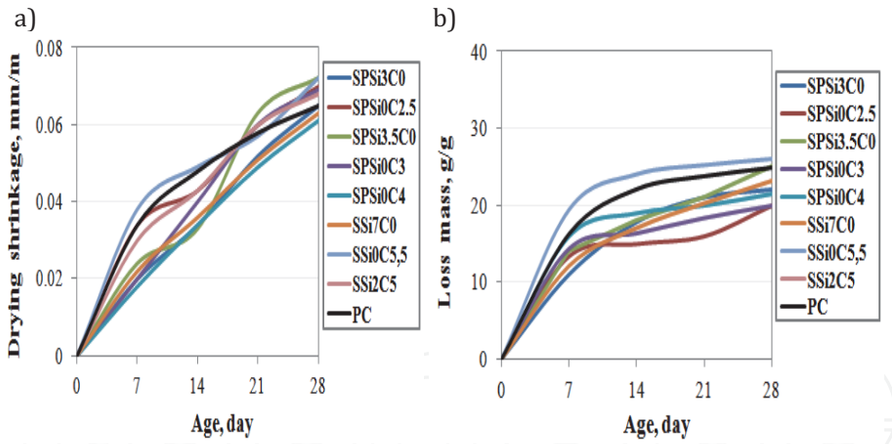

Figure 9.
(a) Drying shrinkage and (b) loss of mass of concrete.

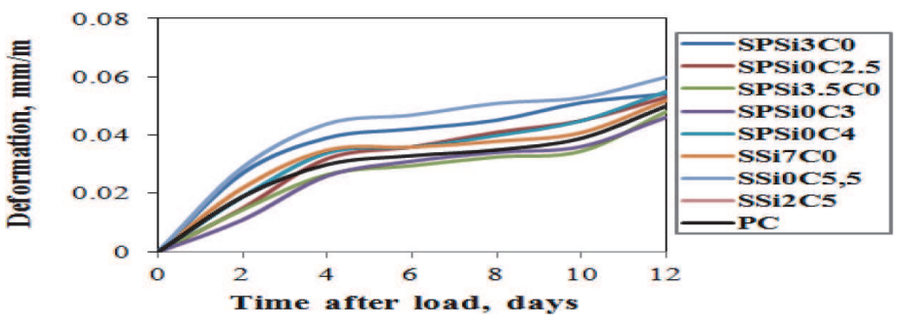

Figure 10.
Creep deformation of concrete.

It has been demonstrated that after 12 days of loading, the creep deformation indices of the concrete samples, based on the PC and alkaline cement, are almost the same for the concrete of common strength classes. For example, when using PC composition of the concrete, the creep deformation value is 0.046 mm/m. When using alkaline cement compositions of concrete, the creep deformation values are within the range of 0.041–0.06 mm/m.

4.8 Modeling of width of crack opening in concrete

A combined effect of such factors as thermal stresses and concrete shrinkage is considered during the crack width investigation in the concrete blocks. The inner stresses (4–9 MPa) and shrinkage deformations (0.061–0.072 mm/m) of the concrete are accepted, taking into account the aforementioned results.

The values obtained (**Figure 11**) testify that the lowest crack width index on the block's surface is typical for proposed SSi7C0 composition of the concrete, with the lowest heat evolution and shrinkage; such a concrete is capable of having a temporary crack opening at the level of 0.03–0.09 mm under the different reinforcement ratios. At the same time, PC composition of the concrete is capable of crack opening at the level of 0.13–0.24 mm under the same conditions depending on the reinforcement rate.

Therefore, the results of concretes obtained, based on the alkaline cement, which has the variable ratio of slag components and the alkali component nature, allow forecasting of their durability. Further, the prospects of widespread use are related to solving ecological problems and reducing energy consumption during production.

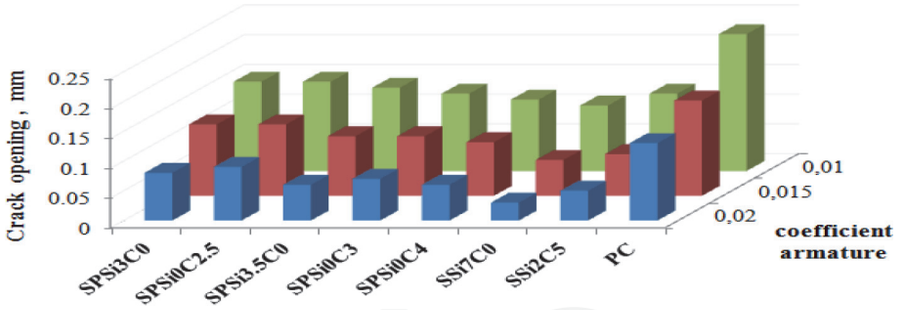

Figure 11.
Simulated crack opening in concrete blocks.

5. Conclusions

On the basis of the investigation carried out and results discussed in this chapter on the use of both alkaline slag Portland cement and alkaline slag cement, and both paste and concrete samples investigated, the following conclusions have been made:

a. The studies showed that independent of the content of slag, nature and amount of alkaline component, alkaline slag Portland cement and alkaline slag cement are characterized by low rates of heat of hydration and low chemical shrinkage compared to Portland cement, by means of reducing of the dispersed phase basicity in alkaline cements and accordingly increasing formation of the low basic silicate hydrates in the composition of hydration products with achieving high compressive strength at the early hardening stages and after 28 days of hardening.

b. The investigations studied a compressive strength, drying shrinkage and creep deformation of concrete based on alkaline cement depending on different clinker/slag ratio, type and content of alkaline component in cement. The study indicated that with the increase of slag content in the cement the concrete strength is reduced in the early age. However, after 14 days of hardening, the concrete strength based on alkaline cement, within the whole range of the slag component content (50–100%), reaches or becomes equal to the strength of concrete based on CEM II/A-S. Indicator drying shrinkage and creep deformation of concrete based on alkaline cement are similar indicators of the concrete based on CEM II/A-S.

c. The study examined temperature distribution, internal stresses and crack opening of modeled concrete blocks based on alkaline cement. It is shown that the use of concrete based on alkaline cement can reduce in twice temperature distribution, both stretching and compressing stresses and reduction of width of crack opening in concrete block compared with concrete based on CEM II/A-S.

Therefore, the obtained investigation results of concretes, based on the alkaline cement, which has the variable ratio of components and the alkaline component nature, allow forecasting of their higher durability, compared with concrete based on CEM II/A-S, according to the heat of evolution and internal stress of concrete at early stages of hardening and their influence on the formation of cracks.

DOI: http://dx.doi.org/10.5772/intechopen.101288

Author details

Oles Lastivka
Scientific Research Institute for Binders and Materials, Kyiv National University of Construction Architecture, Kyiv, Ukraine

*Address all correspondence to: oles.lastivka@gmail.com

References

[1] Azenha M, Faria R, Ferreira D. Identification of early-age concrete temperatures and strains: Monitoring and numerical simulation. Cement and Concrete Composites. 2009;**31**(6): 369-378

[2] Faria R, Azenha M, Figueiras J. Modelling of concrete at early ages: Application to an externally restrained slab. Cement and Concrete Composites. 2006;**28**(6):572-585

[3] Gots V, Pushkarova E, Gonchar O. Synthesis of a durability artificial stone based on fly ash-cement binding systems. In: 18 Ibausil, Weimar; 2012. pp. 1-1079-1-1087

[4] Runova RF, Rudenko II, Troyan VV. High-performance concrete for massive structures. In: 18. Ibausil. Internationale Baustofftagung. – Weimar; Tagunsbericht – Band 2; 12–15 September 2012. pp. 2-0082–2-0089

[5] Barbhuiya SA, Gbagbo JK, Russell MI, Basheer PAM. Properties of fly ash concrete modified with hydrated lime and silica fume. Construction and Building Materials. 2009;**23**:3233-3239

[6] Directive 2012/27/EU of the European Parliament and of the Council of 25 October 2012 on Energy Efficiency, Amending Directives 2009/125/EC and 2010/30/EU and Repealing Directives 2004/8/EC and 2006/32/EC Text with EEA Relevance

[7] Krivenko PV. Alkaline cements, concretes and structures: 50 years of theory and practice. In: Proceedings of the International Conference of Alkali Activated Materials – Research, Production and Utilization. Česka rozvojova agentur, o.p.s., Praha; 2007. pp. 313-331

[8] Krivenko PV, Petropavlovskii ON, Vozniuk GV, Pushkar VI. Constructive properties of the concretes made with alkali-activated cements of new generation. In: First International Conference on Advances of Chemically-Activated Materials (CAM' 2010 - China); Jinan, Shandong, China; 9–12 May 2010. pp. 139-146

[9] Krivenko P, Gots V, Runova R, Rudenko I, Lastivka O. Features of alkali-activated slag Portland cement. In: Proceedings of the 1-st International Conference On the Chemistry of Construction Materials – Berlin; 7–9 October 2013. pp. 453-456

[10] DSTU B V.2.7-181:2009. Alkaline cements. Specifications (National Standard of Ukraine)

[11] Neville A. Properties of Concrete. UK: Longman Group UK Limited, Prentice Hall; 1995. p. 844

[12] Breugel K. Simulation of hydration and formation of structure in hardening cement-based materials [doctoral thesis]. Delft; 1991

[13] Maekawa K, Ishida T, Kishi T. Multi-scale modeling of concrete performance. Integrated material and structural mechanics. Journal of Advanced Concrete Technology. 2003; **1**(2):91-126

[14] Azenha M, Faria R. Temperatures and stresses due to cement hydration on the R/C foundation of a wind tower—A case study. Engineering Structures; **30**(9):2392-2400

[15] ASTM C1608. Standard Test Method for Chemical Shrinkage of Hydraulic Cement Paste. West Conshohocken, PA: ASTM International; 2007. p. 4

[16] BS ISO 1920-8-2009. Testing of concrete – Part 8: Determination of

drying shrinkage of concrete for samples prepared in the field or in the laboratory

[17] BS ISO 1920-9:2009. Testing of concrete – Part 9: Determination of creep of concrete cylinders in compression

[18] Babushkin VI, Matveyev GM, Mchedlov-Petrossyan OP. Thermodynamics of Silicates. Berlin: Springer; 1985

[19] Pryanishnikov OV. High Performance Concrete for Massive Constructions of Building. – Manuscript. Kyiv, Ukraine: Building Materials: 2010. p. 20

[20] Available from: http://elcut.ru

[21] SNIP 2.06.08-87. Longman Group UK Limited. Concrete and Reinforced Concrete Constructions of Hydraulic Building. USSR State Committee; 1988. p. 32

[22] Bazant Z. Prediction of concrete creep and shrinkage: Past, present, and future. Nuclear Engineering and Design. 2001;**203**:27-38